IEEE Open Journal of the Computer Society

Received 19 September 2021; accepted 12 October 2021. Date of publication 19 October 2021;
date of current version 5 November 2021. The review of this article was arranged by Associate Editor Deze Zeng.

Digital Object Identifier 10.1109/OJCS.2021.3121185

Link Scheduling and End-to-End Throughput Optimization in Wireless Multi-Hop Networks

FEI GE [1], LIANSHENG TAN [2,3], WEI ZHANG [1], MING LIU [1], XUN GAO [4], AND JUAN LUO [5] (Member, IEEE)

[1] Computer Science Department, Central China Normal University, Wuhan, Hubei 430079, P. R. China
[2] Discipline of ICT, School of Technology, Environments and Design, University of Tasmania, Hobart, TAS 7001, Australia
[3] Computer Science Department, Huazhong Normal University, Wuhan, Hubei, P. R. China
[4] Electronic Engineering Department, Wuhan University, Wuhan, Hubei 430072, P. R. China
[5] College of Computer Science and Electronic Engineering, Hunan University, Changsha, Hunan 410082, P. R. China

CORRESPONDING AUTHOR: FEI GE (e-mail: feige@mail.ccnu.edu.cn)

This work was supported in part by the National Natural Science Foundation of China under Grants 61672258, 61741204, and 62173157, and in part by the Fundamental Research Funds for the Central Universities of CCNU.

This article has supplementary downloadable material available at https://doi.org/10.1109/OJCS.2021.3121185, provided by the authors.

ABSTRACT The goal of this work is to find appropriate link scheduling schemes to achieve satisfactory end-to-end throughput in wireless multi-hop networks. The algorithm of finding the best path status bitmap is proposed to solve the throughput problem. By analyzing path status, it is found that compressing the path state set can reduce the time complexity. According to this, we describe innovative methods to simplify scheduling of links for long path with large amount of data. Two typical link scheduling schemes with full-duplex radios are proposed, and end-to-end throughput boundary is worked out by analyzing the link capacity and the link active ratio in each scheme. Results illustrate that these schemes may improve end-to-end throughput in wireless multi-hop networks modestly.

INDEX TERMS End-to-end throughput, full-duplex radios, scheduling, wireless multi-hop networks.

I. INTRODUCTION

For decades, topic of wireless network capacity has been extensively explored. The investigations [1], [2] provide basic knowledge about the capacity of fixed or mobile nodes distributed in an area. One node may transmit data to other nodes through a long multi-hop path (LMP) composed of several wireless point-to-point links in large-scale wireless networks. The end-to-end throughput (EET) on such a path (EEToLMP) is related to many factors, such as transmission power, interference and environment, etc. The throughput is studied in combination with routing methods, network size, traffic patterns, offered load, and local radio interactions [3]–[8]. In most wireless communication networks, node works in half-duplex (HD) mode, where simultaneous two-way communications between neighboring nodes require two orthogonal channels. Full-duplex (FD) is impractical without the remarkable progress of self-interference cancellation (SIC) or self-interference suppression (SIS) technology [9]–[11].

The advanced analog/digital signal processing is pushing FD radios to practical systems [12]–[16]. Research [17], [18] shows that a single antenna can realize FD radios in wireless communication systems. Multiple-input multiple-output systems are also jointed with FD radios, where a node having multiple antennas can output and input signals on a channel [19]–[26]. The cellular networks and femto access points benefit from FD radios [27]–[34]. FD technology is also embedded in cognitive radio to improve capacity and spectrum utilization [35]. The results [36] show that the performance of decode-and-forward relaying outperforms that of multi-hop HD relaying in terms of the outage probability. The nodes in relay networks combined with FD radios provide throughput gain [37]–[41].

FD radio improves the capacity on point-to-point link, as well as in relay networks. The situation in wireless multi-hop networks seems to be different. However, recent researches report the potency of FD radios. Wireless multi-hop transmission enhanced by the in-band cut-through method [42] reduces delay and concurrently improves throughput performance. Experiments in the 2.4 GHz ISM band show a throughput gain of up to 3.4× gains on the 4-hop path. The work in [43] considers simultaneous in-band cut-through two-way transmissions through multiple FD relays between

two far-away nodes. By analyzing interference patterns, the authors identify the problem of power amplification at middle nodes, and leverage interference by a loop-back strategy. The experiments show that the two-way throughput gain can achieve 1.6× gains over one-way cut-through systems, and 4.09× gains over the decode-and-forward scheme. In finite-sized multi-hop networks, the results of one or multiple active sessions show 2× gains [44].

One of the main factor limiting the throughput is interference. For example, the radio overlapping of neighboring nodes on LMP brings serious inter-link interferences, which limits data transmission of neighboring nodes. The theoretical and practical results of EEToLMP, when nodes are with HD radios, have been widely recognized. With FD radios, overlapping are still unavoidable. However, FD radios enable node to receive data when sending data, and potentially improve the throughput. The motivation of this work is to investigate how intermediate node with FD radios on LMP contributes to EET.

Apart from inter-link interferences, self-interferences make it difficult for nodes to simultaneously send and receive data at the same time because the interferences may be strong. When distance between active links is long enough, inter-link interferences decrease and the capacities on active links are ensured. The situation of minimizing inter-link interferences is that only one node sends data in the network. However, this makes link active ratio (LAR) on LMP lower, which brings lower EET. Higher LAR will improve the throughput, while very high LAR causes serious interferences. In order to achieve high EEToLMP, the time when a link is active should be arranged. This brings challenge of link scheduling.

One of our main contributions is that we reduce the path statuses by removing replaceable ones on LMP when solving the link scheduling problem of EEToLMP. The other is that we present an approximate but fast solution to the problem. According to it, two scheduling schemes potentially improving the throughput are proposed. Furthermore, We analyze the throughput boundaries in these schemes, and simulate the scheduling procedure of the schemes.

The paper is organized as follows. We first model EEToLMP as an optimization problem in Section II. The algorithm for solving the problem and the link scheduling bitmap to obtain the largest throughput on the path is in Section III. Because the algorithm is time-consuming, and the obtained bitmap is somewhat complicated, we propose an innovative method to speed up the solving procedure in Section IV. The approximate solution is provided and we contribute two fast scheduling schemes in Sections V and VI, respectively. The analysis and simulations of throughput boundaries in Sections VII and VIII show that EEToMTP of these schemes can be higher. We conclude the whole work in Section IX.

II. SYSTEM MODEL

Now consider the problem of maximizing the throughput on LMP in wireless networks, where all nodes are embedded with FD radios. Suppose there are N ($N \geq 4$) nodes in the network and each node is numbered with an unique positive integer number i, $1 \leq i \leq N$. A link l, defined by a sender (node i, $1 \leq i \leq N$) receiver (node j, $1 \leq j \leq N$, $j \neq i$) pair (i, j), may be built between the two nodes. If the transmission range of node i covers node j, the link can be successfully built. If the link is built, it is equivalent to the node pair $l \triangleq (i, j)$. Suppose that there are a number of possible links in the network. One LMP is an ordered set of the links between the source and the destination. The path from the source to the destination is known in advance by the routing algorithm like fixed routing, AODV [45] or DSR [46]. One sender in wireless networks may interference with other nodes whose positions are out of the sender's transmission range. If the interference exists, the interference links are built. An interference link l' between two nodes i and j is also denoted by the node pair (i, j), which means that node j is interfered by node i.

Time is divided into slots, and the duration of a time slot (TS) is long enough to process and transmit a data frame on any link. A node is able to send and receive different frames in a TS. When node i is sending data by the radios, all of its neighboring one-hop nodes will receive the data signal. According to the routing table, only one neighbour j will decode the signal and receive the data for unicast applications. Thus, the link (i, j) is validly built between the two nodes. One link is not always active in the transmission, but active when node i is scheduled to send data to node j. The link is not active in a TS when node i sends data to other nodes or node j receives data from other nodes. If denote the number of total TS by T, the active status of the link in t, $1 \leq t \leq T$, is indicated by binary indicators $a_{(i,j)}(t)$ and $b_{(i,j)}(t)$, respectively, where $a_{(i,j)}(t)$ and $b_{(i,j)}(t)$ are associated to the statuses of nodes i and j. If the link is active in TS t, both the indicators are one, i.e. $a_{(i,j)}(t) = b_{(i,j)}(t) = 1$. Otherwise, at least one of them is zero. For sender i in an unicast application, at most one of its neighbours receives the data in TS t, that is,

$$0 \leq \sum_{1 \leq j \leq N} b_{(i,j)}(t) \leq 1 \tag{1}$$

For receiver j, at most one node sends data in the TS,

$$0 \leq \sum_{1 \leq i \leq N} a_{(i,j)}(t) \leq 1 \tag{2}$$

For interference link $l' = (i, j)$, the corresponding binary variables are also indicated by $\alpha_{(i,j)}(t)$ and $\beta_{(i,j)}(t)$. However, for sender i, more than one and at most $N - 2$ nodes may be interfered by the sender, that is,

$$0 \leq \sum_{1 \leq j \leq N} \beta_{(i,j)}(t) \leq N - 2 \tag{3}$$

In the same way, for receiver j, more than one node may interfere with it. Thus,

$$0 \leq \sum_{1 \leq i \leq N} \alpha_{(i,j)}(t) \leq N - 2 \tag{4}$$

Denote a frame flow crossing one LMP that is constructed by the links between the source and the destination. Denote $h_l = 1$, if the path crosses over link $l \triangleq (i, j)$. The rate x on

link l should not be larger than the average link capacity over the transmission process $\bar{c_l}$, i.e.

$$h_l x \leq \bar{c_l} \tag{5}$$

where $\bar{c_l} = 1/T \sum_{t=1}^{T} c_l(t)$. The capacity on single link l, $c_l(t)$, can be obtained by Shannon's formula.

$$c_l(t) = log_2 \left(1 + \frac{K d_{(i,j)}^{-\gamma} P_i a_{(i,j)}(t)}{I_j(t) + 1}\right) \tag{6}$$

The interferences include self-interference inside the node and all inter-link interference from other nodes. The total power of interference on the node j on link l, after normalized by average background noise power, is

$$I_j(t) = \theta P_j a_{(j,*)}(t) + \sum_{1 \leq k \leq L, k \neq i} K d_{(k,j)}^{-\gamma} \alpha_{(k,j)}(t) P_k \tag{7}$$

where P_i is the transmission power normalized by average background noise power in sending node i on link l, θ is a parameter to denote the residual SIC coefficient (SICC), representing the SIC efficiency. The two-ray propagation model is applied in communications and γ is the loss exponent on the propagation path. Thus, $P_j\theta$ represents the residual self-interference power in node j if a link originated from this node is active. $K d_l^{-\gamma}$ is the path attenuation loss on the path from nodes i and j. The coefficient θ is dependent on the SIC technology adopted by nodes. In general, the coefficient θ is greater than zero, because no perfect SIC technology is developed to date. The coefficient θ is 1 if no SIC is adapted. Thus the coefficient is within the region (0,1]. With the development of advanced signal processing technologies, the coefficient θ can be tiny, like 10^{-11} (-110 dB) [10] or less.

We regard EEToLMP as an optimization problem, whose objective is to maximize the minimum throughput on LMP subject to above constraints, including (1) and (2) due to scheduling method, (3) and (4) due to inter-link interference, routing constraint (5), link capacity constraints (6) and (7). Thus, the optimization problem is formulated by

$$\max\{x : x = \min_l\{\bar{c_l}\}, \ s.t \ \ (1) - (7)\} \tag{8}$$

III. SOLVING THE MODEL

Each link has two statuses, i.e. active and inactive. For a path, the path status describes which link on the path is active or not. Total number of path statuses of one path constructed by L links is 2^L. Denote one path status by one L-dimension vector PS_i, $PS_0 = (0, 0, \ldots, 0, 0)$, $PS_1 = (0, 0, \ldots, 0, 1)$, $PS_2 = (0, 0, \ldots, 1, 0)$, $\cdots$, $PS_{2^L-1} = (1, 1, \ldots, 1, 1)$, where 1 means the link status is active. The path status set, is the set of all path statuses $S_{ps} = \{PS_i, 1 \leq i \leq 2^L - 1\}$ excluding PS_0. Corresponding to PS_i, denote the path capacity on the path by the L-dimension vector PC_i. The path capacity set is denoted by S_{pc}, and $S_{pc} = \{PC_i, 1 \leq i \leq 2^L - 1\}$. The path capacity, PC_i, can be obtained by the path status PS_i and the link capacity formula (6), i.e.

$$PC_i = P(PS_i, \{c_l\}) \tag{9}$$

Algorithm 1: Calculating Best Link Scheduling Bitmap.

Input: node list, link list, total TS number (T)
Output: A_{best}

```
Obtain path status set with 2^L − 1 elements
Calculate EEToLMP under each path status
Obtain combination set S_com (each is with
  T path statuses)
for {each combination}:
  Obtain average link capacity of each
    link over T
  Obtain the path throughput by finding
    the minimum link capacity
  Append the path throughput values to
    a list L_temp
Obtain the largest path throughput by
  finding the maximum throughput in L_temp
return A_best according to the maximum
  throughput
```

Let vectors $a(t) = (a^t_{(1,2)}, a^t_{(2,3)}, \ldots, a^t_{(L,L+1)})$ and $c(t) = (c^t_1, c^t_2, \ldots, c^t_L)$ be the scheduled path status and the corresponding path capacity in the time slot t. Each vector $a(t)$ must be one element of S_{ps}, i.e.

$$a(t) \in S_{ps} \tag{10}$$

When the number of TS is T, there should be T scheduled path statuses and T path capacities. One feasible solution to the problem is a combination including T elements, each of which is one element of S_{ps}. Or say, one solution, A, is a function of T path statuses, i.e. $A = f(S_{ps}, T)$. The solving procedure is to obtain the solution that maximizes $\min_l\{\bar{c_l}\}$ in all feasible ones.

The throughput on multi-hop path obtained by solving the above optimization problem is subject to a few constraints. Within them, the link scheduling scheme describing when nodes send data, plays an important role. The application of FD is expected to increase the variety of scheduling method.

The idea of solving procedure is the exhaustive method. We use Python language to calculate the link scheduling bitmap for achieving the maximum throughput on the path. The core process is described in Algorithm 1.

The time complexity is related to the hop number L and the number of total TS, T, i.e. $O((2^L - 1)^T)$. The total TS number is related to the data volume and the frame size. Therefore, the solving procedure is time-consuming. However, through the following analysis on 3-hop path, we can partly reduce the time complexity of Algorithm 1.

Next we show the solving process of the problem in the scenario where parameters are listed as follows. The hop number is 3. The loss exponent γ is 2, and the radio frequency is set to 800 MHz. The parameter K is from the formula $K = 1/(4\pi/\lambda)^2 \approx 0.00089$. The transmission power P is set to 10 dBm. The distance between neighboring nodes d is set to 500 m. The residual SICC in the node is set to be one.

The number of valid path statuses is $2^L - 1 = 7$. The path status in a TS is in one of the following 7 statuses, (0, 0, 1), (0, 1, 0), (0, 1, 1), (1, 0, 0), (1, 0, 1), (1, 1, 0), (1, 1, 1). On the path, the capacity of one link is the average value of capacities in all TSs. The order of the path status can be neglected here.[1] The combination number of T path statuses is large. However, we will see that the path status may repeat when the transmission time is long. It may be not necessary to consider scheduling the link statuses in all TSs.

The seven path capacity values are calculated according to the seven path statuses. They are (0, 0, 11.799), (0, 11.799, 0), (0, 6.47e-09, 2.321), (11.799, 0, 0), (0.9998, 0, 3.319), (6.47e-09, 2.321, 0), and (6.47e-09, 6.47e-09, 1.913), respectively. The results corresponding to path statuses PS_3, PS_6 and PS_7 depict that a node without SIC can receive data when it is sending data. However, the rate is very low and not practical.

If the number of TSs is 3, the best combination of path status is (PS_1, PS_2, PS_4) by Algorithm 1. The solution to the optimization problem is 3.93, which is 1/3 of the single link capacity. The characteristic of the best combination is that only one link is active in each path status. We can deduce from the result that the solution is still 3.93 when the number of TS is a few times as many as three. And the best combination of path status is several repeat of (PS_1, PS_2, PS_4).

If the number of TSs is 4, the best combination of path status is (PS_1, PS_2, PS_4, PS_7) by Algorithm 1. The solution to the optimization problem is 2.95. This value is about 3/4 times of 3.93, because the throughput in status PS_7 is very low. The reason why PS_7 is chosen is that it at least provides a data path in one TS. The solution is $3m/(3m+1)$ times of 3.93 when $T = 3m + 1 (m \geq 2)$. And the best combination of path status is a few repeat of (PS_1, PS_2, PS_4) and a PS_7.

If the number of TSs is 5, the best combination of path status is $(PS_1, PS_2, PS_4, PS_5, PS_6)$ by Algorithm 1. The solution to the optimization problem is 2.56. The reason why PS_5 and PS_6 is chosen is that it provides the largest throughput in two TSs. The solution is about $3m/(3m+2)$ times of 3.93 when $T = 3m + 2 (m \geq 2)$. The best combination of path status is a few repeat of (PS_1, PS_2, PS_4) and PS_5, PS_6.

From the above results, we can conclude that on the 3-hop path, the throughput is around one third of single link capacity when nodes are without FD radios. The combination of the path statuses is mainly constructed by the repeat of (PS_1, PS_2, PS_4).

Next we consider the solution when nodes are with FD radios and perfect SIC (SICC is set to -20000 dB). The responding link capacity values are obtained, and four values are different from the above, they are PS_3, PS_5, PS_6 and PS_7. Their results are (0, 11.799, 2.321), (0.9998, 0, 3.319), (11.799, 2.321, 0), and (0.9998, 2.321, 1.913), respectively.

If the number of time slots is 3, the solution to the optimization problem is also 1/3 of the single link capacity. The combination of path status achieving the throughput, from our software, is (PS_1, PS_2, PS_4). By careful compare, we find that the combination (PS_1, PS_3, PS_6) can do this. However, it cannot be extended that the solution is still 3.93 when T is a few times as many as three TSs. The results from Algorithm 1 show that the combination is mostly constructed by PS_1, PS_3 and PS_6, and the solution is larger than 3.93. For example, the solution is 4.18 when the number of TS is 18, and the combination is PS_1, PS_1, PS_1, PS_1, PS_1, PS_1, PS_2, PS_2, PS_2, PS_3, PS_3, PS_6, PS_6, PS_6, PS_6, PS_6, PS_6, and PS_6, respectively. These results show modestly improved throughput in this case.

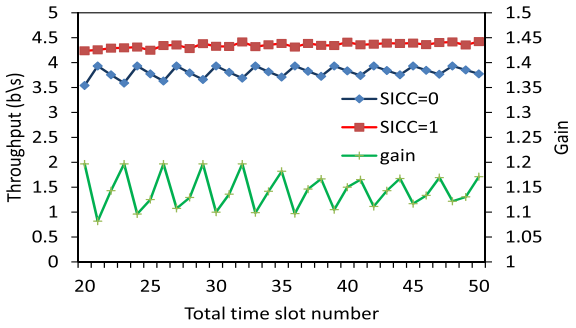

FIGURE 1. Throughput and gain values on the 3-hop path.

If the number of TSs is 4, the solution to the optimization problem is 3.53. This value is still larger than 2.95 when without SIC. The corresponding combination of path status is different, that is, (PS_1, PS_3, PS_4, PS_6). If the number of TSs is 5, the solution to the optimization problem is 3.29, larger than 2.56 when without SIC. The corresponding combination of path status is $(PS_1, PS_1, PS_2, PS_6, PS_6)$. If the number of TSs is 6, the solution to the optimization problem is 3.93. The corresponding combination of path status is $(PS_1, PS_1, PS_2, PS_2, PS_4, PS_4)$.

For more TSs, we plot the throughput results and the gains when T changes from 20 to 50 in Fig. 1. The results show the slight gain (about 1.15) by perfect FD radios in this scenario.

IV. REDUCTION OF PATH STATUSES

The time complexity of Algorithm 1 is related to the size of PS. Reducing the size can speed up the solving procedure. The above processes show that the best combination of path statuses is just made up of a part of all path statuses. On the premise that the throughput does not decrease, we can remove "redundant" path statuses.

Next we define the replaceable path status in a single TS.

Definition 1: Let $v, w \in S_{ps}$ and $v \neq w$, in combination C including v, the throughput is X_1. In a new combination where w replaces v, the throughput is X_2. When $X_2 \geq X_1$, we say that v is a replaceable path status by w in the combination $v \overset{C}{\leftarrow} w$. If v is a replaceable path status by w in all combinations, we say that v is globally replaced by w, $v \leftarrow w$.

The procedure to find all globally replaceable path status is listed in Algorithm 2.

[1] In real transmission, the order should be arranged according to the time.

Algorithm 2: Finding Replaceable Path Statuses.

Input: pathstatuslist, lkcapall
Output: replacedpathstatus,replacedpathstatusid

```
// The variable pathstatuslist is
   assigned to the path status list.
   The variable lkcapall is assigned
   to the path capacity list. The
   variable replacedpathstatus is
   assigned to the replaceable path
   status list. The variable
   replacedpathstatusid is assigned
   to the id of the replaceable path
   status list.
replacedpathstatus=[]
replacedpathcap=[]
replacedpathstatusid=[]
for {an element in lkcapall indexed by i}:
 tempv1=lkcapall[i]
 for {an element in lkcapall indexed by j}:
  if j!=i:
   tempv2=lkcapall[j]
   replacesign=0
   for {a link indexed by k}:
    if tempv2[k]>=tempv1[k]:
     replacesign=replacesign+1
   if replacesign==L:
    tmp=[pathstatuslist[i],
     pathstatuslist[j]]
    append tmp to replacedpathstatus
    tem=[lkcapall[i],lkcapall[j]]
    append tmp to replacedpathcap
    append i to replacedpathstatusid
```

In the ideal situation where SICC=0, two path statuses are replaceable on the 3-hop path, i.e. $PS_2 \leftarrow PS_3$ and $PS_4 \leftarrow PS_6$. After the replacement, the size of S_{ps} reduces from 7 to 5. The time complexity of Algorithm 1 decreases.

To understand why the replacement is feasible, we may consider the path capacity corresponding to the replaceable path status. In the above example, when the status is PS_2=(0,1,0), the corresponding path capacity is (0, 11.799, 0). When the status is PS_3=(0,1,1), the corresponding path capacity is (0, 11.799, 2.321). The link capacity does not decrease if PS_2 is replaced by PS_3. Therefore, the replacement does not influence the final result. In fact, SIC leads to the feasible replacement. Generally, we have the following theorem.

Theorem 1: With perfect SIC, if there is one path status just having one active link and the link is not the last hop, the path status is a replaceable one.

Proof: Denote the path status just having one active link (the link is not the last hop) by $v = (\alpha_1, \alpha_2, \ldots, \alpha_L)$. It is characterized by $\alpha_i = 1$ and $\alpha_j = 0$, $1 \le i \le L-1$, $j \in \{1, 2, \ldots, L\} - \{i\}$. The corresponding link capacities are $c_i^v > 0$ and $c_j^v = 0$, $1 \le i \le L-1$, $j \in \{1, 2, \ldots, L\} - \{i\}$.

Consider another path status w where $\alpha_i = \alpha_{i+1} = 1$ and $\alpha_j = 0$, $1 \le i \le L-1$, $j \in \{1, 2, \ldots, L\} - \{i, i+1\}$. That is, links i and $i+1$ become active. The corresponding link capacities are $c_i^w > 0$, $c_{i+1}^w > 0$ and $c_j^w = 0$, $1 \le i \le L-1$, $j \in \{1, 2, \ldots, L\} - \{i, i+1\}$. With perfect SIC, it has $c_i^w = c_i^v$ and $c_{i+1}^w > c_{i+1}^v = 0$.

Therefore, if w replaces v in any combination including v, the throughput on the path does not reduce. ■

In a path with L links, the path status number in Algorithm 1 can be decreased from $2^L - 1$ to $2^L - L$ by the Theorem 1. For example, when $L = 4$, it reduces to 12. The algorithm's time complexity changes from original $O(15^T)$ to current $O(12^T)$.

Beside self-interference, inter-link interference makes small capacity. Therefore, if two links close to each other are simultaneously active, the inter-link interference may result in low capacity on both links. For example, the path capacities responding to the path status PS_5 is (0.9998, 0, 3.319). The capacity on the first link in PS_5 is quite less than that on the first link in PS_4. The capacity on the third link in PS_5 is quite less than that on the third link in PS_1. This implies that the path status PS_5 may be replaced by the PS_4 and PS_1. However, the replacement requires two slot times. That is, if there are two path statuses PS_5 in two TSs, they can be replaced by one PS_4 and one PS_1. In this case, we can define replaceable path status in multiple slots.

Definition 2: The path status $v, w_j \in S_{ps}$, $j = 1, \ldots, J$ and $v \ne w_j$, in combination C_k including $M (M > 1)$ path status v, the throughput is X_1. In a new combination where M w_j replaces M v, the throughput is X_2. When $X_2 >= X_1$, we say that v is a replaceable path status in M time slots by $\{w_j\}$, $j = 1, \ldots, J$ in the combination, $v \xleftarrow[M]{C_k} \{w_j\}$.

The algorithm to find the replaceable path status in 2 TSs is listed in Algorithm 3.

With perfect SIC, one path status may be replaceable on the 3-hop path. In the above scenario, $PS_5 \xleftarrow[2]{C_k} \{PS_4, PS_1\}$. In combinations wherever two PS_5 appear, PS_4 and PS_1 can replace them. In the same way, three PS_7 in a combination can be replaced. The solution is similar if we remove PS_5 and PS_7 in the combination. The time complexity of Algorithm 1 for the solution reduces to $O(3^T)$. After replacement, in this case, the solution is the same with that before replacement.

On the path where there are more than 3 hops, the path status like (1001) may not be replaced. The reason may be that the distance between the two active links is large enough, and the inter-link interference is relatively small.

V. APPROXIMATE SOLUTION

The above case analysis shows that most path statuses are replaceable. The results give the enlightenment that, in the 3-hop path, we just need to arrange the three path statuses. When the balance of the three link capacities in all TSs is ensured, the optimal link scheduling is obtained. The balancing procedure of the scheduling is to increase the capacity of the link with smallest average capacity in the former TSs. Some steps in the procedure are listed in Table 1. PS_6 is selected in the first TS, and $\bar{c}_3$ is the smallest. In next TS, PS_1 is selected

Algorithm 3: Finding Replaceable Path Status in 2 TSs.

Input: pathstatuslist, lkcapall
Output: replacedpathstatus,replacedpathstatusid

```
replacedpathstatus=[]
replacedpathcap=[]
replacedpathstatusid=[]
for {an element in lkcapall indexed by i}:
 tempv1=lkcapall[i]
 foundsign=0
 for {an element in lkcapall indexed by j}:
  if foundsign==1:
   break
  for {an element in lkcapall indexed by j2}:
   if foundsign==1:
    break
   if j!=i and j2!=i:
    tempv2=lkcapall[j]
    tempv2_2=lkcapall[j2]
    replacesign=0
    for k in range(0,L):
     if tempv2[k]+tempv2_2[k]>=2*tempv1[k]:
      replacesign=replacesign+1
    if replacesign==L:
     append [x[i],x[j],x[j2]] to
      replacedpathstatus
     append [lkcapall[i],lkcapall[j],
      lkcapall[j2]] to replacedpathcap
     append i to replacedpathstatusid
     foundsign=1
```

TABLE 1. The Scheduling Process

TS	PS no.	PS	$\bar{c}_1, \bar{c}_2, \bar{c}_3$	x
1	PS_6	1,1,0	11.799,2.321,0	0
2	PS_1	0,0,1	5.9,1.160,5.9	1.16
3	PS_3	0,1,1	3.933,4.707,4.707	3.933
4	PS_6	1,1,0	5.9,4.11,3.53	3.53
5	PS_1	0,0,1	4.72,3.2882,5.184	3.288
6	PS_3	0,1,1	3.933,4.707,4.707	3.933
7	PS_6	1,1,0	5.057,4.366,4.034	4.034
...	...	...	...	...

to enlarge $\bar{c}_3$, which makes that $\bar{c}_2$ is the smallest. In next TS, PS_3 is selected to enlarge $\bar{c}_2$. According to the procedure, the best PS sequence can be obtained. The PS sequence is the best scheduling scheme in the transmission.

This method can have the optimal path status combination to the problem and have better time complexity than the above algorithms. However, for the long path with a lot of hops, the method is a little more complex. Next we consider an approximate method for the long path. The idea is to divide the long path into groups according to the interference between links. In each group, we use the above method.

If one link on the path has little interference with another link, these two links are put in different groups. For example, when l_1 is far away from l_5, they are put in different groups. Thus, l_1 and l_5 can be active in the same time.

The first step of the solution is to find the suitable distance for avoiding large inter-link interference. The method to judge this is to see whether one path status like 00010010000 can be replaced by 00010000000 and 00000010000 in two time slots. If no, it means that the inter-link interference is small. If yes, it means that the inter-link interference is large. Then, increase the distance between the two active links, and see whether the path status 00010001000 can be replaced by 0001000000 and 0000000100. Repeat this process until the distance is long enough. After grouping the links, the second step is to arrange the link active order in each group.

slot \ node	1	2	3	4	5	6	7	8	9	10	11	12
1	1											
2	2	1										
3	3	2	1									
4	4	3	2	1								
5	5	4	3	2	1							
6	6	5	4	3	2	1						
7	7	6	5	4	3	2	1					
8	8	7	6	5	4	3	2	1				
9	9	8	7	6	5	4	3	2	1			
10	10	9	8	7	6	5	4	3	2	1		
11	11	10	9	8	7	6	5	4	3	2	1	
12	12	11	10	9	8	7	6	5	4	3	2	1
13	13	12	11	10	9	8	7	6	5	4	3	2
14	14	13	12	11	10	9	8	7	6	5	4	3
15	15	14	13	12	11	10	9	8	7	6	5	4
16	16	15	14	13	12	11	10	9	8	7	6	5
17	17	16	15	14	13	12	11	10	9	8	7	6
18	18	17	16	15	14	13	12	11	10	9	8	7

FIGURE 2. A snapshot in SS1, where neighboring nodes can simultaneously send frame in one TS. The number in the cross unit is the frame number.

VI. SCHEDULING TRANSMISSIONS

In this section, we list four scheduling schemes on the path predefined by any routing algorithm, and study how they affect EEToLMP. Three require FD radios, and the left one is a traditional benchmark when making comparative research.

A. SCHEME 1

Scheduling scheme 1 (SS1) means that all intermediate nodes on the path (excluding source node and destination node) receive and send data simultaneously in any TS. Thus, the constraint (11) of intermediate nodes on the path should be satisfied.

$$a_i(t) = a_{i+1}(t) = 1, 1 \le i \le N-3, i \le t \le T^{(1)} \qquad (11)$$

A part of the scheduling procedures in the scheme are shown in Fig. 2. In the figure, the horizontal direction and vertical direction respectively represent the number of nodes from 1 to 12, and TS from 1 to 18, respectively. The number in the cross grid refers to the frame sequence sent by corresponding node in the corresponding TS. The path includes 8 nodes, and the frame is assigned a sequence number (Sno). Node 1 sends Frame 1 to node 2, which receives it in the first TS. In the second frame, node 2 sends frame 1 to node 3, and node 1 send Frame 2 to node 2. In the later TSs, more and more nodes send and receive frames in one slot.

node / slot	1	2	3	4	5	6	7	8	9	10	11	12
1	1											
2		1										
3			1									
4	2			1								
5		2			1							
6			2			1						
7	3			2			1					
8		3			2			1				
9			3			2			1			
10	4			3			2			1		
11		4			3			2			1	
12			4			3			2			1
13	5			4			3			2		
14		5			4			3			2	
15			5			4			3			2
16	6			5			4			3		
17		6			5			4			3	
18			6			5			4			3

FIGURE 3. A snapshot in SS2, where neighboring nodes do not simultaneously send frame in one TS.

node / slot	1	2	3	4	5	6	7	8	9	10	11	12
1	1											
2	2	1										
3		2	1									
4			2	1								
5	3			2	1							
6	4	3			2	1						
7		4	3			2	1					
8			4	3			2	1				
9	5			4	3			2	1			
10	6	5			4	3			2	1		
11		6	5			4	3			2	1	
12			6	5			4	3			2	1
13	7			6	5			4	3			2
14	8	7			6	5			4	3		
15		8	7			6	5			4	3	
16			8	7			6	5			4	3
17	9			8	7			6	5			4
18	10	9			8	7			6	5		

FIGURE 4. A snapshot in SS3, where neighboring nodes may simultaneously send different frame in one TS.

Node i, $1 \le i \le N-1$, sends frames in TS t when t, $1 \le t \le T^{(1)}$, satisfies

$$i \le t \le T^{(1)} - i + 1$$

The sequence s, $1 \le s \le S$, sent by the node in this TS, is

$$s = t - i + 1$$

The total number of the TSs, $T^{(1)}$, for finishing transmitting S frames on the path with N nodes, is obtained by

$$T^{(1)} = S + N - 2$$

B. SCHEME 2

The idea in SS2 is to separate the sending nodes on the path by enough distance. In this scheme, the node is without FD radios, and the distance of 3 hops are reserved for simultaneously sending nodes. For example, nodes 1, 4 and 7 simultaneously send data in TS 10, as shown in Fig. 3.

If node i, $1 \le i \le N-1$, is active in TS t, $1 \le t \le T^{(2)}$, the necessary condition (12) should be satisfied

$$t\%3 = i\%3, i \le t \le T^{(2)} - N + i + 1 \tag{12}$$

where % is a modulo operator. The frame number, sent by node i in TS t, is obtained by

$$s = \lceil (t - i + 1)/3 \rceil$$

where $\lceil x \rceil$ means the ceiling integer of x. For example, node 5 sends frames $s = \lceil (5 - 5 + 1)/3 \rceil = 1$ and $s = \lceil (8 - 5 + 1)/3 \rceil = 2$ in TSs 5 and 8, respectively.

The total number of the TSs, $T^{(2)}$, to complete the transmission of S frames on N node path, is the sum of two parts. The first part is the duration the first frame required from the source to the destination, i.e. $N-1$. The second one is for transmitting the following $S-1$ frames. One additional frame takes additional 3 slots, and $S-1$ frames take $(S-1)$ slots according to this schedule scheme. Therefore, the total TSs required to complete the transmission is

$$T^{(2)} = (S-1) \times 3 + (N-1) = 3S + N - 4$$

C. SCHEME 3

In SS1, inter-link interferences are serious, although nodes works with FD radios. In SS2, inter-link interferences are less, but FD radios is not applied. We provide SS3, where neighboring nodes may have the opportunity to simultaneously send frames in one TS. The scheduling procedure is shown in Fig. 4. For example, in the 6-th TS, neighboring nodes 5 and 6 send frames 2 and 1, respectively. In the same slot, neighboring nodes 1 and 2 send frames 4 and 3, respectively. Nodes 3 and 4 remain silent. In next TS, neighboring nodes 6 and 7 and neighboring nodes 2 and 3 send frames together. The space between nodes 2 and 5 in slot 6, or between nodes 3 and 6 in TS 7, is three hops, to avoid serious inter-link interferences.

We are still considering transmitting large amounts of data on the path with N nodes. Nodes 1 and N are the source node and the destination node respectively. The active node i in the transmission on the path should meet one of the two conditions, i.e. (13) and (14) in TS t

$$t\%4 = i\%4, i \le t \le T^{(3)} - N + i + 1 \tag{13}$$

$$(t-1)\%4 = i\%4, i \le t \le T^{(3)} - N + i + 1 \tag{14}$$

Sno s sent by node i if TS t satisfies (13) is

$$s = \lceil (t - i + 1)/4 \rceil \times 2 - 1$$

Sno s sent by node i, if TS t satisfies (14), is

$$s = \lceil (t - i + 1)/4 \rceil \times 2$$

This relationship indicates that the frames sent by nodes in a TS are usually pairs. Two frames in one pair are sent by neighboring nodes. For example, in TS 10, there are three pairs, i.e. frames 1 and 2, frames 3 and 4, frames 5 and 6,

slot \ node	1	2	3	4	5	6	7	8	9	10	11	12
1	1	1										
2			1	1								
3	2	2			1	1						
4			2	2			1	1				
5	3	3			2	2			1	1		
6			3	3			2	2			1	1
7	4	4			3	3			2	2		
8			4	4			3	3			2	2
9	5	5			4	4			3	3		
10			5	5			4	4			3	3
11	6	6			5	5			4	4		
12			6	6			5	5			4	4
13	7	7			6	6			5	5		
14			7	7			6	6			5	5
15	8	8			7	7			6	6		
16			8	8			7	7			6	6
17	9	9			8	8			7	7		
18			9	9			8	8			7	7

FIGURE 5. **Neighboring links may be simultaneously active and send the same frame in one TS in SS4.**

which are sent by 6 nodes. From the node's point of view, it usually sends two frames in two consecutive slots, and keeps silent in the next two slots. For instance, node 1 sends frames in slots 1, 2, 5, 6, etc., and remains silent in slots 3, 4, 7, 8, etc., until all frames are transmitted.

When the number of all frames, S, is an odd, it requires $N-1$ slots to transmit the last frame on N node path. The other $S-1$ frames need $2\times(S-1)$ TSs due to the scheduling method in SS3. Therefore, the total time is the sum of the above two values, i.e. $(S-1)\times 2+N-1$. When S is an even, the total transmission time includes three parts. The last frame requires $N-1$ slots on N node path. The second last frame requires 1 slot for a node. The other $S-2$ frames need $2\times(S-2)$ slots due to the schedule method for a node. The sum, $(S-2)\times 2+1+N-1$, is the overall transmission time. Thus, total TSs for finishing S frames on N node path, is

$$T^{(3)}=\begin{cases}(S-1)\times 2+N-1=2S+N-3 & S\%2=1\\ (S-2)\times 2+N=2S+N-4 & S\%2=0\end{cases} \tag{15}$$

D. SCHEME 4

With cut-through FD radios, SS4 is feasible, whose scheduling procedure is shown in Fig. 5. In this scheme, two neighboring nodes send one frame simultaneously. For example, in TS 3, nodes 1 and 2 send Sno 2 to node 3. In the same time, nodes 5 and 6 send Sno 1 from node 5 to node 7. The space between nodes 2 and 5 should be large enough to eliminate the impact of inter-link interferences. Therefore, two adjacent nodes are grouped. For example, nodes 1 and 2 are grouped to group 1. Node i is in the group $\lceil i/2\rceil$. The total group number is $\lceil (N-1)/2\rceil$. The difference between SS4 and SS3 lies in that if neighboring nodes send the same frame in one TS.

Consider a lot of frame data on an LMP with N nodes, where nodes 1 and N are the source and the destination, respectively. If node i, $1\le i\le N-1$, in TS t sends data in the transmission, the following conditions should be satisfied

$$t\%2=\lceil i/2\rceil\%2 \tag{16}$$

$$\lceil i/2\rceil\le t\le T^{(4)}-\lceil (N-1)/2\rceil+\lceil i/2\rceil+1$$

The operation $\lceil i/2\rceil$ groups neighboring nodes into a team.

Total TSs, for transmitting S frames on N-node path, is

$$T^{(4)}=(S-1)\times 2+\lceil (N-1)/2\rceil \tag{17}$$

where $\lceil (N-1)/2\rceil$ is the slots required for a frame to transmit a frame from the source to the destination, and $(S-1)\times 2$ is the time a node required to transmit $S-1$ frames. Correspondingly, in this scheme, Sno that node i sends in TS t is

$$s=\lceil (t-\lceil i/2\rceil+1)/2\rceil$$

Briefly, the key factors to differ these schemes are self-interference and inter-link interference. Table 2 describes the level of interferences in four schemes.

TABLE 2. **Interferences in Four Schemes**

Scheme	self-interference	inter-link interference
SS1	heavy	heavy
SS2	zero	light
SS3	heavy	light
SS4	heavy	light

VII. THROUGHPUT BOUNDARY

Inevitably, the scheduling scheme will influences the transmission procedure. Next, we will analyze the boundary under each SS. When all links are active in SS1, the end-to-end throughput is bounded in Theorem 2.

Theorem 2: The throughput boundary for transmitting S frames on LMP with N nodes in SS1 is

$$x^{(1)}=\frac{S}{S+N-2}\min_{1\le i\le N-1}c_i^{(1)} \tag{18}$$

where

$$c_i^{(1)}=log_2\left(1+\frac{Kd_i^{-\gamma}P_i}{\theta P_{i+1}+Kd_{i+1}^{-\gamma}P_{i+2}+1}\right) \tag{19}$$

Proof: The size of a frame is L_{Frame} bits. In SS1, the capacity on link l_i in any TS, according to (6), is less than (19). The duration for transmitting a frame on link l_i is $L_{Frame}/c_i^{(1)}$. Select the maximum duration to be the value of a TS, i.e.

$$D^{(1)}=\max_{1\le i\le N-1}\frac{L_{Frame}}{c_i^{(1)}}=\frac{L_{Frame}}{\min_{1\le i\le N-1}c_i^{(1)}} \tag{20}$$

The average active times on link l_i is the proportion of total frame number S to total TS number T for transmitting S frames, i.e. $S/T^{(1)}=(T^{(1)}-N+2)/T^{(1)}=S/(S+N-2)$ The maximum throughput on multi-hop path is $x^{(1)}=\frac{S}{S+N-2}\times\frac{L_{Frame}}{D^{(1)}}$ Substitute (20) into it, the capacity boundary (18) is obtained. ■

The throughput, if the links are scheduled by SS2, can be obtained by Theorem 3.

Theorem 3: The throughput boundary for transmitting S frames on LMP with N nodes in SS2 is

$$x^{(2)} = \frac{S}{3S+N-4} \min_{1\le i\le N-1} c_i^{(2)} \tag{21}$$

where

$$c_i^{(2)} = log_2\left(1 + Kd_i^{-\gamma} P_i\right) \tag{22}$$

Proof: The link active times is $S/(3S+N-4)$ and the maximum capacity on link i is $c_i^{(2)}$. Therefore, the throughput boundary is $\frac{S}{3S+N-4} \min_{1\le i\le N-1} c_i^{(2)}$. ■

The throughput boundaries, if nodes are scheduled according to SS3 and SS4, can be obtained by Theorems 4 and 5.

Theorem 4: The throughput boundary for transmitting S frames on LMP with N nodes in SS3 is

$$x^{(3)} = \begin{cases} \frac{S}{2S+N-3} \min_{1\le i\le N-1} c_i^{(3)} & S\%2 = 1 \\ \frac{S}{2S+N-4} \min_{1\le i\le N-1} c_i^{(3)} & S\%2 = 0 \end{cases} \tag{23}$$

where

$$c_i^{(3)} = \begin{cases} log_2\left(1 + Kd_i^{-\gamma} P_i\right) & s\%2 = 1 \\ log_2\left(1 + \frac{Kd_i^{-\gamma} P_i}{\theta P_{i+1}+1}\right) & s\%2 = 0 \end{cases} \tag{24}$$

Proof: In this scheme, neighboring links have the chance to be active in one TS. If the data required to transmit is S frames,the total active slot number for each link is S.

Now consider the average LAR on each link. The overall slot number $T^{(3)}$ is obtained by (15). The duration for sending a frame on the active link is $L_{Frame}/c_i^{(3)}$. The duration of a TS $D^{(3)}$ should be long enough, so we select the maximum duration, like (20). We first consider that S is an odd number.

If $S\%2 = 1$, the average active times on link l_i in this scheme is the proportion of S to $T^{(3)}$, i.e. $S/T^{(3)} = \frac{S}{2S+N-3}$. The throughput on multi-hop path is by $x^{(3)} = \frac{S}{T^{(3)}} \frac{L_{Frame}}{D^{(3)}} = \frac{S}{2S+N-3} \min_{1\le i\le N-1} c_i^{(3)}$.

If $S\%2 = 0$, the average active ratio is slightly different. The throughput on multi-hop path is by $x^{(3)} = \frac{S}{2S+N-4} \min_{1\le i\le N-1} c_i^{(3)}$

The capacity on active link in this scheme is related to the SIC technology. We analyze the situation when frame number is an odd number firstly.

If $S\%2 = 1$, the total number of TSs when a node is active is composed by two parts. One is the odd TS number, which is $(S+1)/2$. The other is the even TS number, which is $(S-1)/2$. When a node transmits a frame numbered odd on corresponding link, the maximum capacity is $log_2(1 + Kd_i^{-\gamma} P_i)$ When a node transmits a frame numbered even on corresponding link, the maximum capacity is $log_2(1 + \frac{Kd_i^{-\gamma} P_i}{\theta P_{i+1}+1})$. Therefore, the capacity is (24).

If $S\%2 = 0$, it is similar to get the capacity. The total number of TSs when a node is active is composed by two parts. One is the odd TS number, which is $S/2$. The other is the even TS number, which is also $S/2$. The capacity when an odd frame is sent is different with that when an even frame is sent. However, the capacity is also (24). ■

The result show that LAR in this scheme is better than that in SS2, and the the throughput on multi-hop path can be enhanced. In SS4, two nodes are grouped to be one team, and the data may cross one team in a TS.

Theorem 5: The throughput boundary for transmitting S frames on LMP with N nodes in SS4 is

$$x^{(4)} = \frac{S}{2S + \lceil (N-1)/2 \rceil - 2} \min_{1\le i\le N-1} c_i^{(4)} \tag{25}$$

where

$$c_i^{(4)} = \begin{cases} log_2\left(1 + Kd_i^{-\gamma} P_i\right) & i\%2 = 1 \\ log_2\left(1 + \frac{Kd_i^{-\gamma} P_i}{\theta P_{i+1}+1}\right) & i\%2 = 0 \end{cases} \tag{26}$$

Proof: The duration of one TS $D^{(4)}$ is selected according to

$$L_{Frame}/min_{1\le i\le N-1} c_i^{(4)}$$

The process to obtain $c_i^{(4)}$ is the same as that in SS3. The result is also similar with that in SS3. The average LAR is $S/T^{(4)}$, where $T = 2S - 2 + \lceil (N-1)/2 \rceil$ according to (17). Therefore, the throughput boundary (25) is obtained. ■

VIII. SIMULATION RESULTS

A simulator [47] is designed to simulate the transmission scheduling process. It can simulate link scheduling processes and obtain corresponding throughput. We integrate four SSs into the simulator. Comparison between simulation results and analysis results would show whether the SSs are feasible in the transmission on the multi-hop path, and whether the throughput analyses are reasonable.

The simulator is programmed by Python 3.5. The main object in the simulator is the node, which is composed of several modules, including the radio module, which is used to set the radio-related parameters, such as transmission power, SICC, antenna gains, average noise power and radio frequency; The store module, which stores the generated frames if the node is the source, and stores the frames to be forwarded if the node is a relay; The forwarding module for storing the forwarding table; The scheduling module, configured to decide which TS the node should use in the channel; The time module for storing TS; The location module to set and store the node's position; The identification (ID) module to store and set the number of the numbered node. The important attribute in nodes is slotseq, specifying the time slot used by nodes.

One frame is composed with a header segment and a data segment. The former includes five fields, namely slottime, sourcenodeID, destinationnodeID, lastnodeID, and nextnodeID. The field slottime stores current TS when the frame is generated by the source node. The pair, sourcenodeID and destinationnodeID, stores IDs of the source node and the destination node. It is designed to store the end-to-end data flow information as soon as the data is framed. When a node receives a frame, it should check whether it is the destination or not from the header. If so, it stores the frame. Otherwise, it should forward the frame to next hop according to the routing table. The fields lastnodeID and nextnodeID are used

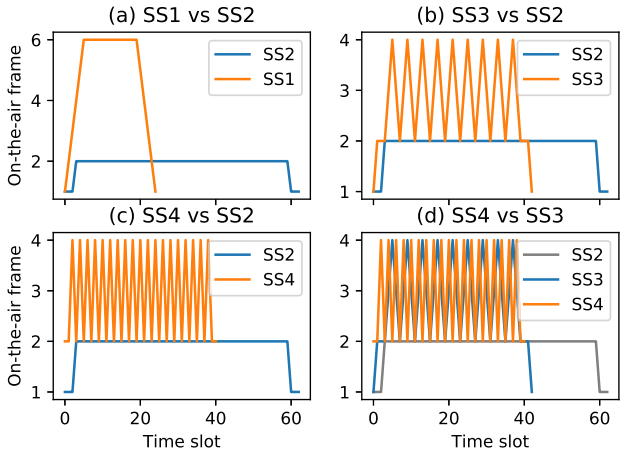

FIGURE 6. Number of on-the-air frames on the six-hop path.

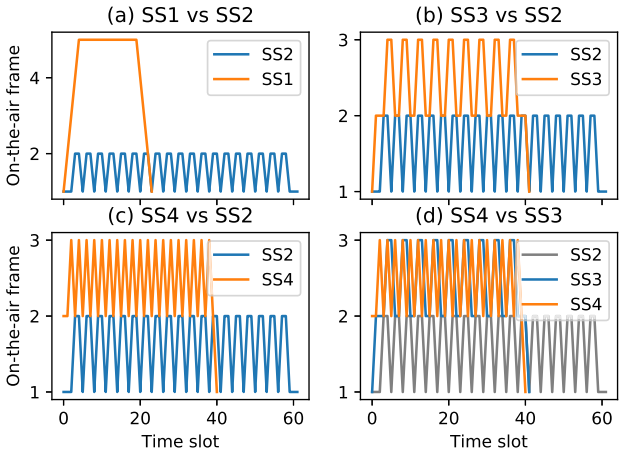

FIGURE 7. Number of on-the-air frames on the six-hop path.

for forwarding frames. When a node receives a frame, it can judge from the field nextnodeID whether the node is the next hop for the frame on the path. If so, the node stores the frame in its buffer. Otherwise, it drops the frame. The field lastnodeID is used to specify the node who sends the frame. For a source node, the source node ID is filled in this field. Before a frame is forwarded by a relay node, the fields lastnodeID and nextnodeID should be changed. The data segment in the frame contains fields like the byte number and the check code. It should be noted that the frame size is fit for the duration of TS and the minimum one-hop capacity.

The algorithms describing the implementation of four SSs and the transmission process in the simulator are omitted due to limit space. It is believed that these schemes can be realized on multi-hop path. We understand LAR through total on-the-air frame number (TOFN) sent by nodes on the path in the transmission process. Fig. 6 plots TOFN in the transmission on the 7-node path. Subfigures a, b and c compare TOFNs in SSs 1, 3 and 4 to those in SS2. Subfigure (d) compares the values in SS3 and SS4 to those in SS2.

The change of TOFN can be divided to three phases, the starting phase, the stationary phase and the ending phase. In SS1, TOFN in each TS increases from 1 to 6 in the starting phase, decreases from 6 to 1 in the ending phase, and maintains 6 in the stationary phase. On the 7-node path, LAR in SS1 approximates to 100%. In SS2, TOFN in each TS increases from 1 to 2 in the starting phase, decreases from 2 to 1 in the ending phase, and maintains 2 in the stationary phase. On the 7-node path, LAR in this scheme approximates to 1/3. In SS3, TOFN in the stationary phase jumps according to the route 2-3-4-3-2-3-4-3-2. On the 7-node path, LAR in SS3 is about 1/2. We can find the cause of this phenomenon in Fig. 2. In SS4, TOFN in the stationary phase jumps according to the route 2-4-2-4-2. On the 7-node path, LAR in SS4 approximates to 1/2. The reason for this phenomenon can be found in Fig. 2.

However, TOFN may be different when the number of nodes on LMP changes. In Fig. 7 (a-c), we compare the values

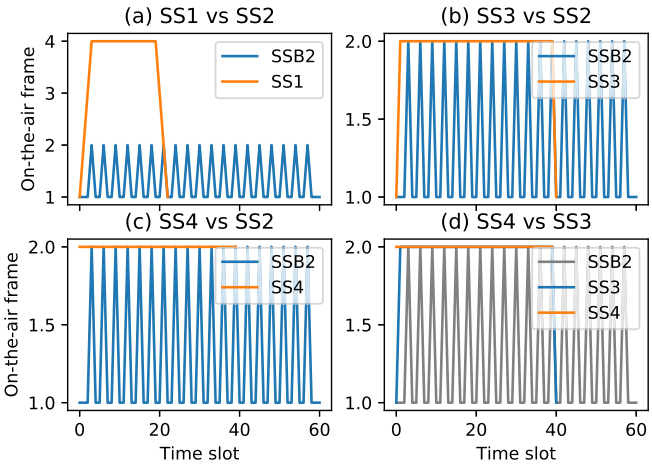

FIGURE 8. Number of on-the-air frames on the four-hop path.

in SSs 1, 3 and 4 to those in SS2. In Fig. 7(d), we compare the values in SS3 to those in SS4. In SS2, TOFN in the stationary phase is not fixed, but jumps according to the route 1-2-2-1-2-2-1. On the 7-node path, LAR in SS2 approximates to 1/3. In schemes 3 and 4, TOFN in the stationary phase is still jumping, and LAR is about 1/2.

TOFN in SSs 3 or 4 does not always change and is fixed if node number on the path satisfies $(N-1)\%4=0$. If the number of nodes is 5, in Fig. 8 (a-c), we compare the values in SSs 1, 3 and 4 to those in SS2. In Fig. 8(d), we compare the values in SS3 to those in SS4, and find that TOFN is always 2 in the stationary phase in SSs 3 and 4. Although TOFN in each scheme changes, LAR in stationary phase is similar.

The scheduling schemes influence link active rate, average link capacity, data transmission and further end-to-end throughput on the path. If the network parameters are fixed and the path is generated by a routing algorithm, then EE-ToLMP is determined by SS. For example, LARs in the four schemes approximate to 1, 1/3, 1/2, and 1/2, respectively, when the amount of data is large enough. We present several

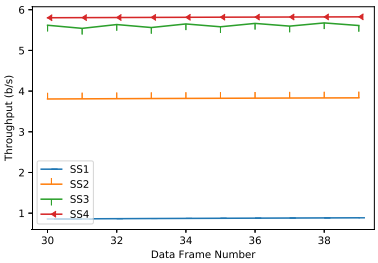

FIGURE 9. Throughput with number of data frames.

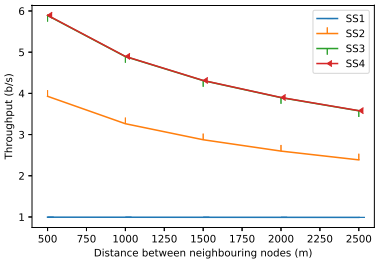

FIGURE 10. Throughput at different distances.

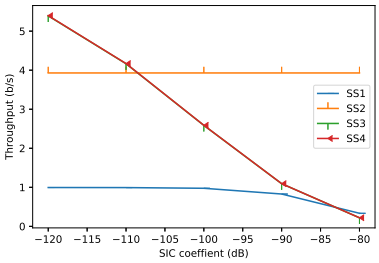

FIGURE 11. Throughput with different SIC coefficients.

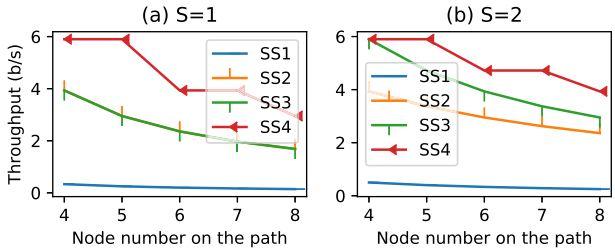

FIGURE 12. Throughput under different number of nodes.

scenarios, and compare the end-to-end throughput values[2] in four SSs.

Consider a path in wireless networks where nodes are distributed with equal distance, and all nodes have identical parameters. A two-ray propagation model is applied in communications, and the loss exponent γ is 2. The radio frequency is set to 800 MHz, and then the parameter K is 0.00089, from the formula $K = 1/(4\pi/\lambda)^2$. The transmission power P is set to 10 dBm. The residual SICC is set to be ideally zero. The path consists of $N = 7$ nodes (six hops) and the data is divided to $S = 1000$ frames. The distance between neighboring nodes d is set to 500 m. Unless otherwise specified, the following results are on the basis of these settings.

The length of the path will influence the throughput. In SS1, the throughput decreases $1/(S + N - 1)$ when one hop is added on the path. If $S >> N$, this decrease is very slight. For example, when $S = 1000$, the decrease is about 0.001. If the data is small, like $S = 1$, the throughput seriously decreases with increasing hops. The main reason for the decrease is the decrease of the LAR. Fig. 12(a) shows the results when the path contains 4, 5, 6, 7 and 8 nodes. In SS1, the values are 0.33, 0.25, 0.20, 0.17, and 0.14, respectively. The throughput values in schemes 2 and 3 have identical trends, and both of them decrease on the long path. The results also show that SS3 can not improve the throughput in this case. The reason is that one frame of data can not provide the chance of application of FD radios. The throughput results, when $S = 2$, are plotted in Fig. 12(b). The throughput values in SS3 are larger than those in SS2, because two neighboring nodes may simultaneously send frames. Furthermore, the throughput values in 12(b) are not less than the values in Fig. 12(a). The throughput results in the first three schemes decrease when one hop is added. SS4 is special, and the values decrease by every two hops. Meanwhile, the cut-through FD brings shorter transmission time and corresponding higher throughput value on LMP in this scenario.

The large hop count on the path greatly reduces the link active ratio and the throughput, especially when data is small. In the same time, more data increases the link active ratio. Let's take the results in SS3 as an example. Fig. 9 shows the results with data volume in a range from 5 to 50 frames on the path with 7 nodes. Although the throughput increases with the increase of the frame number, it finally approximates to an upper value. This results reflect that the link active ratio has an upper boundary. From the above, we know that these boundaries should be 1, 1/3, 1/2 and 1/2, respectively. The necessary condition for reaching the boundary is that the data volume is large enough, that is, $S >> N$.

In addition to LAR, the capacity on the active link also influences EEToLMP. The capacity of an active link in SS1 is limited by interference from the next hop node and self-interference. The interference is so heavy that the capacity can not exceed one, even when LAR is close to 100%. Therefore, EEToLMP can not exceed 1, i.e. $x^{(1)} < \frac{S}{S+N-2} < 1$.

The capacity of an active link in SS2 is not influenced by the neighboring next hop node because the scheme makes the node inactive in the TS. The capacity of the active link is related to the distance between neighboring nodes. Although the link is not always active, LAR is close to 1/3 if the amount of data is large. Therefore, EEToLMP is bounded by $x^{(2)} < \frac{1}{3} log_2(1 + 9(100/d)^2)$.

[2]The word "throughput" in this section refers to "throughput boundary".

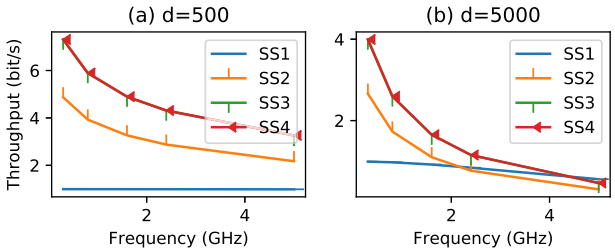

FIGURE 13. **Throughput on different frequency.**

In SS3 or SS4, LAR is close to 1/2. The capacity of an active link is obtained by $log_2(1 + 9(100/d)^2)$. Therefore, EEToLMP is bounded by $x^{(3)} < 0.5log_2(1 + 9(100/d)^2)$.

We plot all results of EEToLMP in this scenario in Fig. 10. It seems that there are only three curves in this figure. In fact, four curves are drawn, and two of which overlap. That is to say, the values in schemes 3 and 4 are very similar. It can be seen from the figure that the longer the distance is, the smaller the throughput of any scheme is. Generally speaking, the throughput in SS3 is larger than that in SS2.

SIC has a great impact on FD performance, further on EEToLMP. The following texts describes how SICC θ influences the multi-hop throughput in these schemes.

EEToLMP in SS2 will not change with the change of SICC, but its value will change in other schemes. Fig. 11 shows the results when SICC changes from -120 dB to -80 dB. It is found that in the scenario, the throughput values in schemes 3 and 4 decrease very quickly.

The radio frequency has an impact on EEToMTP. The frequency will change the capacity of a link by changing the parameter K. Higher frequency brings lower K, which leads to lower power received in the receiver. Therefore, the link capacity is lower. In the four schemes, the trend of throughput also goes down with the increase of radio frequency, as Fig. 13 shows. It is found in Fig. 13(a) that the value is the maximum one in schemes 3 or 4 with 300 MHz radio frequency, and the value is about 1 with 5 GHz.

Throughput decreases by increasing the distance between adjacent nodes. The reason is that the link capacity has been reduced. Fig. 13(b) shows the corresponding results when the distance d is 5000. By comparing two results, it is found that no matter which scheme is adopted, the shorter the distance is, the greater the throughput will be. Moreover, the value under the radio frequency 5 GHz is greatly decreased.

IX. CONCLUSION

Maximizing EEToLMP in large-scale wireless networks is an optimization problem subject to many constraints including link scheduling. Nodes with FD radios enable more SSs in the end-to-end transmission. We give the algorithm to solve this problem, and illustrate the best combination of path statuses on 3-hop path. We reduce the size of path status set by removing the replaceable path statuses, in order to decrease the time complexity of the algorithm. We describe the approximate method to solve the problem. Four SSs are depicted in detail. We find that the scheduling process, together with FD radios, influence the boundary of EET on multi-hop path.

We simulate these SSs in a simulator, verify that the schemes can be realized, and observe the whole scheduling process in each scheme. Under different network settings and node parameters, we compare the results of these four schemes. These results provide intuitive knowledge about how SS3 or SS4 is dominant in multi-hop wireless networks.

In the future, when using FD radio for end-to-end transmission, we should consider the trade-off between the node's energy consumption and the throughput. The energy consumption may limit the throughput increase. Furthermore, the end-to-end delay reduced by FD radios on multi-hop path may be noticed, especially in delay sensitive applications.

REFERENCES

[1] P. Gupta and P. R. Kumar, "The capacity of wireless networks," *IEEE Trans. Inf. Theory*, vol. 46, no. 2, pp. 388–404, Mar. 2000.
[2] M. Grossglauser and D. Tse, "Mobility increases the capacity of ad hoc wireless networks," *IEEE/ACM Trans. Netw.*, vol. 10, no. 4, pp. 477–486, Aug. 2002.
[3] J. Li, C. Blake, D. S. De Couto, H. I. Lee, and R. Morris, "Capacity of Ad Hoc wireless networks," in *Proc. 7th Annu. Int. Conf. Mobile Comput. Netw.*, 2001, pp. 61–69.
[4] D. S. J. De Couto, D. Aguayo, J. Bicket, and R. Morris, "A high-throughput path metric for multi-hop wireless routing," in *Proc. 9th Annu. Int. Conf. Mobile Comput. Netw.*, New York, NY, USA, 2003, pp. 134–146.
[5] M. Kodialam and T. Nandagopal, "Characterizing the capacity region in multi-radio multi-channel wireless mesh networks," in *Proc. 11th Annu. Int. Conf. Mobile Comput. Net.*, New York, NY, USA, 2005, pp. 73–87.
[6] P. C. Ng and S. C. Liew, "Throughput analysis of IEEE 802.11 multi-hop ad hoc networks," *IEEE/ACM Trans. Netw.*, vol. 15, no. 2, pp. 309–322, Apr. 2007.
[7] Y. Gao, D. M. Chiu, and J. C. S. Lui, "Determining the end-to-end throughput capacity in multi-hop networks: Methodology and applications," *Meas. Model. Comput. Syst.*, vol. 34, no. 1, pp. 39–50, 2006.
[8] S. Rezaei, M. Gharib, and A. Movaghar, "Throughput analysis of IEEE 802.11 multi-hop wireless networks with routing consideration: A general framework," *IEEE Trans. Commun.*, vol. 66, no. 11, pp. 5430–5443, Nov. 2018.
[9] M. Jain *et al.*, "Practical, real-time, full duplex wireless," in *Proc. 17th Annu. Int. Conf. Mobile Comput. Netw.* 2011, pp. 301–312.
[10] D. Bharadia, E. McMilin, and S. Katti, "Full duplex radios," in *Proc. ACM SIGCOMM Conf.*, 2013, pp. 375–386.
[11] E. M. Fouda, S. Shaboyan, A. Elezabi, and M. A. Eltawil, "Application of Ica on self-interference cancellation of in-band full duplex systems," *IEEE Wireless Commun. Lett.*, vol. 9, no. 7, pp. 924–927, Jul. 2020.
[12] H. Vogt, G. Enzner, and A. Sezgin, "State-space adaptive nonlinear self-interference cancellation for full-duplex communication," *IEEE Trans. Signal Process.*, vol. 67, no. 11, pp. 2810–2825, Jun. 2019.
[13] D. Kim, H. Lee, and D. Hong, "A survey of in-band full-duplex transmission: From the perspective of phy and mac layers," *IEEE Commun. Surv. Tut.*, vol. 17, no. 4, pp. 2017–2046, Oct.–Dec. 2015.
[14] Z. Zhang, X. Chai, K. Long, A. V. Vasilakos, and L. Hanzo, "Full duplex techniques for 5G networks: Self-interference cancellation, protocol design, and relay selection," *IEEE Commun. Mag.*, vol. 53, no. 5, pp. 128–137, May 2015.
[15] J. Marašević, T. Chen, J. Zhou, N. Reiskarimian, H. Krishnaswamy, and G. Zussman, "Full-duplex wireless: Algorithms and rate improvement bounds for integrated circuit implementations," in *Proc. 3rd Workshop Hot Topics Wireless*. New York, NY, USA, 2016, pp. 28–32.
[16] T. Chen *et al.*, "Full-duplex wireless based on a small-form-factor analog self-interference canceller: Demo," in *Proc. 17th ACM Int. Symp. Mobile Ad Hoc Netw. Comput.*, New York, NY, USA, 2016, pp. 357–358.

[17] A. Sabharwal, P. Schniter, D. Guo, D. W. Bliss, S. Rangarajan, and R. Wichman, "In-band full-duplex wireless: Challenges and opportunities," *IEEE J. Sel. Areas Commun.*, vol. 32, no. 9, pp. 1637–1652, Sep. 2014.
[18] S. Hong *et al.*, "Applications of self-interference cancellation in 5G and beyond," *IEEE Commun. Mag.*, vol. 52, no. 2, pp. 114–121, Feb. 2014.
[19] D. G. Wilson-Nunn, A. Chaaban, A. Sezgin, and M. S. Alouini, "Antenna selection for full-duplex MIMO two-way communication systems," *IEEE Commun. Lett.*, vol. 21, no. 6, pp. 1373–1376, Jun. 2017.
[20] A. Almradi and K. A. Hamdi, "On the outage probability of MIMO full-duplex relaying: Impact of antenna correlation and imperfect CSI," *IEEE Trans. Veh. Technol.*, vol. 66, no. 5, pp. 3957–3965, May 2017.
[21] M. Zhou, L. Song, Y. Li, and X. Li, "Simultaneous bidirectional link selection in full duplex MIMO systems," *IEEE Trans. Wireless Commun.*, vol. 14, no. 7, pp. 4052–4062, Jul. 2015.
[22] W. Ouyang, J. Bai, and A. Sabharwal, "Leveraging one-hop information in massive MIMO full-duplex wireless systems," *IEEE/ACM Trans. Netw.*, vol. 25, no. 3, pp. 1528–1539, Jun. 2017.
[23] R. Sultan, L. Song, K. G. Seddik, and Z. Han, "Full-duplex meets multiuser MIMO: Comparisons and analysis," *IEEE Trans. Veh. Technol.*, vol. 66, no. 1, pp. 455–467, Jan. 2017.
[24] R. Malik and M. Vu, "Optimal transmission using a self-sustained relay in a full-duplex MIMO system," *IEEE J. Sel. Areas Commun.*, vol. 37, no. 2, pp. 374–390, Feb. 2019.
[25] Z. Qian, F. Wu, Z. Zheng, K. Srinivasan, and N. B. Shroff, "Concurrent channel probing and data transmission in full-duplex MIMO systems," in *Proc. 18th ACM Int. Symp. Mobile Ad Hoc Netw. Comput.*, New York, NY, USA, 2017, pp. vol. 15, pp 1–10.
[26] T. Zheng, H. Wang, Q. Yang, and M. H. Lee, "Safeguarding decentralized wireless networks using full-duplex jamming receivers," *IEEE Trans. Wireless Commun.*, vol. 16, no. 1, pp. 278–292, Jan. 2017.
[27] S. Goyal, P. Liu, S. S. Panwar, R. A. Difazio, R. Yang, and E. Bala, "Full duplex cellular systems: Will doubling interference prevent doubling capacity?," *IEEE Commun. Mag.*, vol. 53, no. 5, pp. 121–127, May 2015.
[28] K. Shen, R. Khosravi-Farsani, and W. Yu, "Capacity limits of full-duplex cellular network," *IEEE Inf. Theory Workshop*, pp. 1–5, 2019, doi: 10.1109/ITW.2018.8613531.
[29] Z. Tong and M. Haenggi, "Throughput analysis for full-duplex wireless networks with imperfect self-interference cancellation," *IEEE Trans. Commun.*, vol. 63, no. 11, pp. 4490–4500, Nov. 2015.
[30] J. Marasevic, J. Zhou, H. Krishnaswamy, Y. Zhong, and G. Zussman, "Resource allocation and rate gains in practical full-duplex systems," *IEEE/ACM Trans. Netw.*, vol. 25, no. 1, pp. 292–305, Feb. 2017.
[31] M. Duarte *et al.*, "Design and characterization of a full-duplex multiantenna system for WiFi networks," *IEEE Trans. Veh. Technol.*, vol. 63, no. 3, pp. 1160–1177, Mar. 2014.
[32] M. Hua, L. Yang, C. Pan, and A. Nallanathan, "Throughput maximization for full-duplex UAV aided small cell wireless systems," *IEEE Wireless Commun. Lett.*, vol. 9, no. 4, pp. 475–479, Apr. 2020.
[33] I. Avgouleas, N. Pappas, D. Yuan, and V. Angelakis, "Probabilistic cooperation of a full-duplex relay in random access networks," *IEEE Access*, vol. 5, pp. 7394–7404, 2017.
[34] S. Xiao *et al.*, "Joint uplink and downlink resource allocation in full-duplex ofdma networks," in *Proc. IEEE Int. Conf. Commun.*, 2016, pp. 1–6.
[35] Y. Liao, L. Song, Z. Han, and Y. Li, "Full duplex cognitive radio: A new design paradigm for enhancing spectrum usage," *IEEE Commun. Mag.*, vol. 53, no. 5, pp. 138–145, May 2015.
[36] T. K. Baranwal, D. S. Michalopoulos, and R. Schober, "Outage analysis of multihop full duplex relaying," *IEEE Commun. Lett.*, vol. 17, no. 1, pp. 63–66, Jan. 2013.
[37] K.-C. Hsu, K. C.-J. Lin, and H.-Y. Wei, "Full-duplex delay-and-forward relaying," in *Proc. 17th ACM Int. Symp. Mobile Ad Hoc Netw. Comput.*, New York, NY, USA, 2016, pp. 221–230.
[38] I. Krikidis, H. A. Suraweera, P. J. Smith, and C. Yuen, "Full-duplex relay selection for amplify-and-forward cooperative networks," *IEEE Trans. Wireless Commun.*, vol. 11, no. 12, pp. 4381–4393, Dec. 2012.
[39] Z. Chen, T. Q. S. Quek, and Y. C. Liang, "Spectral efficiency and relay energy efficiency of full-duplex relay channel," *IEEE Trans. Wireless Commun.*, vol. 16, no. 5, pp. 3162–3175, May 2017.
[40] D. Bharadia and S. Katti, "FastForward: Fast and constructive full duplex relays," in *Proc. ACM Conf. SIGCOMM*. New York, NY, USA, 2014, pp. 199–210.
[41] M. S. Amjad and F. Dressler, "Software-based in-band full duplex relays for ieee 802.11a/g/p: An experimental study," in *Proc. IEEE Wireless Commun. Netw. Conf.*, 2021, pp. 1–7.
[42] B. Chen, Y. Qiao, O. Zhang, and K. Srinivasan, "Airexpress: Enabling seamless in-band wireless multi-hop transmission," in *Proc. 21st Annu. Int. Conf. Mobile Comput. Netw.*, New York, NY, USA, 2015, pp. 566–577.
[43] L. Chen, F. Wu, J. Xu, K. Srinivasan, and N. Shroff, "BiPass: Enabling end-to-end full duplex," in *Proc. 23rd Annu. Int. Conf. Mobile Comput. Netw.*, NY, USA, 2017, pp. 114–126.
[44] X. Qin *et al.*, "Impact of full duplex scheduling on end-to-end throughput in multi-hop wireless networks," *IEEE Trans. Mobile Comput.*, vol. 16, no. 1, pp. 158–171, Jan. 2017.
[45] C. Perkins, E. Beldingroyer, and S. Das, "RFC 3561-Ad Hoc on-demand distance vector (AODV) routing," Accessed Jan. 20, 2019. [Online]. Available: http://www.ietf.org/rfc/rfc3561.txt
[46] D. B. Johnson, D. A. Maltz, and J. Broch, "Ad hoc networking," Boston, MA, USA: Addison-Wesley Longman Publishing Co., Inc., 2001, ch. *DSR: The Dynamic Source Routing Protocol for Multihop Wireless Ad Hoc Networks*, pp. 139–172. [Online]. Available: http://dl.acm.org/citation.cfm?id=374547.374552
[47] F. Ge, "Simulation of scheduling schemes in full duplex embedded wireless networks," Accessed: Aug. 24, 2021. [Online]. Available: https://codeocean.com/capsule/0ce0e364 47534c13 8e4fe4e7dfa2ae46/

FEI GE received the B.S. and M.S. degrees in measurement and automatic devices, and the Ph.D. degree in communication and information system from Wuhan University, Wuhan, China, in 1997, 2001, and 2005, respectively.

He is currently an Associate Professor with the Computer Science Department, Central China Normal University, Wuhan, China. From 2008 to 2010, he was a Postdoctoral Research Fellow with The College of Physical Science and Technology, Central China Normal University. From 2010 to 2011, he was a Research Fellow with the Department of Electrical Engineering, City University of Hong Kong, Hong Kong. He has authored or coauthored more than 40 papers in international journals and conference proceedings, including IEEE, ACM, and Elsevier journals. His research interests include embedded system, transmission control, Internet of Things, wireless network communications, and data processing.

Dr. Ge is an ACM Member and a Member of China Computer Federation. He acts as a reviewer for international jounals and the TPC member for conferences. His award includes Hubei Science and Technology Progress Award.

LIANSHENG TAN received the Ph.D. degree in mathematical science from Loughborough University, Loughborough, U.K., in 1999. He is currently with the Discipline of ICT, School of Technology, Environments and Design, University of Tasmania, Hobart, TAS, Australia, and he was a Professor with the Department of Computer Science, Central China Normal University, Wuhan, China.

He was a Research Fellow with the Research School of Information Sciences and Engineering, The Australian National University, Canberra, ACT, Australia, from 2006 to 2009, and a Postdoctoral Research Fellow with the School of Information Technology and Engineering, University of Ottawa, Ottawa, ON, Canada, in 2001. He also held a number of visiting research positions with the Loughborough University, University of Tsukuba, Tsukuba, Japan, City University of Hong Kong, Hong Kong, and University of Melbourne, Melbourne, VIC, Australia. He has authored or coauthored more than 130 papers in international journals and conference proceedings, including more than 20 in IEEE and ACM journals and two monographs with Elsevier and Taylor & Francis. His research interests include cloud computing, Internet of Things, computer networks, and wireless sensor networks.

Dr. Liansheng Tan is currently the Editor-in-Chief of the *Journal of Computers*, the Editor of the *International Journal of Computer Networks and Communications*. He was the Editor of the *Dynamics of Continuous, Discrete & Impulsive Systems (Series B: Applications & Algorithms)* during 2006–2008, and the Editor of the *International Journal of Communication Systems*.

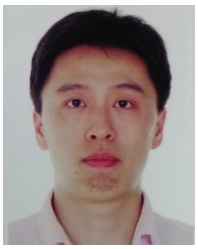

WEI ZHANG received the Ph.D. degree from Central China Normal University, Wuhan, China, in 2008. He is currently a Lecturer with the School of Computer, Central China Normal University. His current research interests include resource allocation, performance evaluation, and optimization of computer communication networks.

MING LIU received the Ph.D. degree in system analysis science from the Huazhong University of Science and Technology, Wuhan, China, in 2009. He is currently a Professor with the School of Computer, Central China Normal University, Wuhan, China. From 2012 to 2013, he was a Visiting Scholar with the Department of Computer Sciences, Georgia State University, Atlanta, GA, USA.

He has authored or coauthored more than 60 papers in a variety of academic journals and conference proceedings. His research interests include cloud computing, Internet of Things, and wireless sensor networks.

XUN GAO received the B.S. in electronic information engineering, the M.S. degree in signal and information processing, and the Ph.D. degree in communication and information system from Wuhan University, Wuhan, China, in 2003, 2005, and 2009, respectively.

He is currently an Associate Professor with Electronic Information School, Wuhan University. From 2012 to 2013, he was a Visiting Associate Research Scholar with the Department of Electrical Engineering, Princeton University, Princeton, NJ, USA. His research interests include Internet of Things, network communications, and battery-efficient low power design.

Prof. Gao is an Integrated Circuit Technical Committee Member and a Senior Member of the China Institute of Communications. His awards and honors include the National Innovation and Entrepreneurship Mentoring Award by the Ministry of Education of China, Google Faculty Award and Hubei Science and Technology Progress Award.

JUAN LUO (Member, IEEE) received the bachelor's degree in electronic engineering from the National University of Defense Technology, Changsha, China, in 1997, and the master's and Ph.D. degrees in communication and information system from Wuhan University, Wuhan, China, in 2000 and 2005, respectively.

She is currently a Professor and a Doctoral Supervisor with the College of Computer Science and Electronic Engineering, Hunan University, Changsha, China. From 2008 to 2009, she was a Visiting Scholar with the University of California Irvine, Irvine, CA, USA.

Prof. Luo has authored or coauthored more than 70 papers in international journals and conference proceedings. Her research interests include the Internet of Things, cloud computing, and middleware. She is a Member of ACM and SIGCOM. She is also a Senior Member of China Computer Federation.